

Disorders of the Nervous System

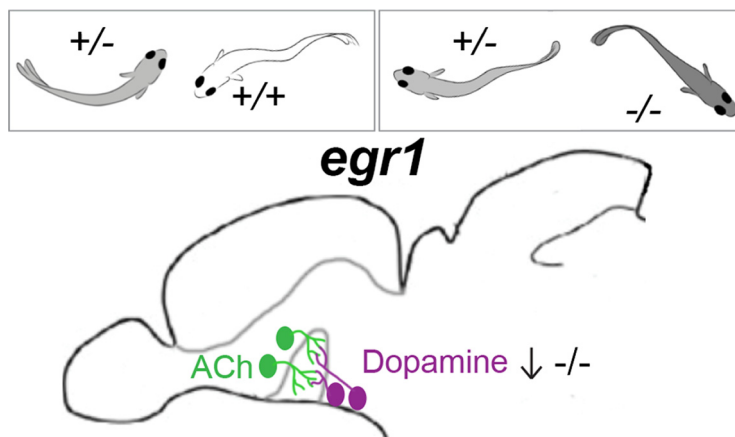
# Egr1 Is Necessary for Forebrain Dopaminergic Signaling during Social Behavior

Alexandra Tallafuss,<sup>1</sup> Sarah J. Stednitz,<sup>2</sup> Mae Voeun,<sup>1</sup> Anastasia Levichev,<sup>1</sup> Johannes Larsch,<sup>3</sup> Judith Eisen,<sup>1</sup> and Philip Washbourne<sup>1</sup>

<https://doi.org/10.1523/ENEURO.0035-22.2022>

<sup>1</sup>Institute of Neuroscience, University of Oregon, Eugene, OR 97403, <sup>2</sup>Queensland Brain Institute, Brisbane, QLD 4072, Australia, and <sup>3</sup>Max Planck Institut für Neurobiologie, Martinsried, D-82152, Munich Germany

## Visual Abstract



## Abstract

Finding the link between behaviors and their regulatory molecular pathways is a major obstacle in treating neuropsychiatric disorders. The immediate early gene (IEG) *EGR1* is implicated in the etiology of neuropsychiatric disorders, and is linked to gene pathways associated with social behavior. Despite extensive knowledge of *EGR1* gene regulation at the molecular level, it remains unclear how *EGR1* deficits might affect the social component of these disorders. Here, we examined the social behavior of zebrafish with a mutation in the homologous gene *egr1*. Mutant fish exhibited reduced social approach and orienting, whereas other sensorimotor behaviors were unaffected. On a molecular level, expression of the dopaminergic biosynthetic enzyme,

### Significance Statement

*Egr1* is an immediate early gene (IEG) linked to neuropsychiatric disorders, particularly those with social components. However, the role it plays in control of social behavior remains elusive. We found that zebrafish with a mutation in the *egr1* gene present deficits in social approach and orienting behavior. Furthermore, *egr1* mutants have reduced tyrosine hydroxylase (TH) expression, particularly in dopaminergic neurons of the preoptic area (POA) synaptically connected to neurons already identified within a social circuit. Our study provides evidence of a role for *egr1* in establishing social behavior, and adds to our understanding of the underlying circuitry.

tyrosine hydroxylase (TH), was strongly decreased in TH-positive neurons of the anterior parvocellular preoptic nucleus. These neurons are connected with basal forebrain (BF) neurons associated with social behavior. Chemogenetic ablation of around 30% of TH-positive neurons in this preoptic region reduced social attraction to a similar extent as the *egr1* mutation. These results demonstrate the requirement of *Egr1* and dopamine signaling during social interactions, and identify novel circuitry underlying this behavior.

**Key words:** dopamine; preoptic area; social behavior; zebrafish

## Introduction

Intraspecies interaction, or social behavior, is a widespread phenomenon among animals. It is considered to be beneficial for reasons of predator evasion, reproduction and cooperative foraging (Fernald, 2012). Brain regions, neuronal circuits, as far as they have been characterized, and even genes regulating social behavior are conserved and follow similar basic principles across vertebrates. Therefore, understanding the neuronal circuits and gene networks that underlie social behavior in animal models may provide information pertinent to disorders that compromise human social behavior.

One of the most studied genes with dysregulated expression in disorders with a social component is the immediate early gene (IEG) *EGR1*. In fact, this gene has been evaluated as a biomarker for certain neuropsychiatric disorders (Cattane et al., 2015; Czéh et al., 2016). *EGR1* has been linked to stress-related mood disorders, schizophrenia, and major depressive disorder (Covington et al., 2010; Kimoto et al., 2014). In addition, gene expression studies and gene network modeling have identified *EGR1* as part of a synaptic gene node disrupted in brains of individuals with autism spectrum disorder (ASD; Liu et al., 2016). *EGR1* can perform this nodal function as it is a critical component, similar to other activity-induced transcription factors such as *FOS*. They regulate downstream late-response genes involved in neuronal physiology by dynamically activating a molecular response cascade consisting of a wide range of genes (Duclot and Kabbaj, 2017)

Studies in mouse models also point to a role for *Egr1* in social behaviors. Social defeat stress, a common depression model, reduces *Egr1* expression in the prefrontal

cortex (Covington et al., 2010), confirming *Egr1* as biological marker for stress-related depressive disorder. Furthermore, antisense-mediated knock-down of *Egr1* reduces male rat social interaction (Stack et al., 2010), identifying a direct contribution of *Egr1* to social behavior. Conversely, viral-mediated *Egr1* overexpression prevents castration-induced deficits in male rat social interactions (Dossat et al., 2017). Similarly, the optogenetic stimulation of cells in the prefrontal cortex increases *Egr1* expression and induces anti-depressant effects (Covington et al., 2010). In zebrafish, social deprivation results in down-regulation of four genes, including *egr1* (Anneser et al., 2020). In addition, in cichlid fish, *egr1* is specifically induced in the preoptic area (POA) as a response to recognition of social opportunity and ascension to dominance (Burmeister et al., 2005). In response to *Egr1* expression, gonadotropin-releasing hormone (GNRH)-expressing neurons undergo physiological changes and exhibit an increase in GNRH mRNA and protein expression (Burmeister et al., 2005). Thus, studies in both the human patient population and vertebrate models suggest a role for *Egr1* in the organization and functioning of brain circuits that support social behavior.

The *Egr1* gene encodes a transcription factor with upregulatory and downregulatory effects on a multitude of target genes. Around 9000 genes, 54% of genes annotated in the Encyclopedia of DNA Elements (ENCODE) project, contain at least one *Egr1* binding motif in their promoter region (Duclot and Kabbaj, 2017). Despite this widespread potential to bind to promoters, *Egr1* shows a bias toward genes involved in regulating synaptic function and plasticity (Duclot and Kabbaj, 2017). For example, *Egr1* is recruited to the *PSD-95* promoter in response to NMDA receptor activation (Qin et al., 2015). Also, the presynaptic plasticity gene *Synapsin1* has long been known to be regulated by *Egr1* (Thiel et al., 1994). In addition to regulating these synaptic proteins, *Egr1* binds to the gene encoding tyrosine hydroxylase (TH), a biosynthetic enzyme for catecholaminergic neurotransmitters (NTs), often involved in response to emotional stress (Papanikolaou and Sabban, 2000; Stefano et al., 2006). Further, the expression of *th* and *egr1* are tightly correlated in response to sensory deprivation in zebrafish (Kress and Wullmann, 2012), suggesting that *Egr1* modulates expression of TH-synthesized NTs in an activity-dependent manner. Nevertheless, it remains unclear whether *Egr1* regulates gene expression in specific neural circuits that contribute to social behavior.

Development of robust social behavior was recently described in the zebrafish (Dreosti et al., 2015; Larsch and Baier, 2018; Stednitz and Washbourne, 2020) and a region of the basal forebrain (BF) necessary for this behavior was identified (Stednitz et al., 2018). Here, we examine

Received January 24, 2022; accepted March 12, 2022; First published March 28, 2022.

The authors declare no competing financial interests.

Author contributions: A.T., J.L., J.E., and P.W. designed research; A.T., S.J.S., M.V., A.L., J.L., and P.W. performed research; A.T., S.J.S., M.V., A.L., J.L., and P.W. analyzed data; A.T., J.E., and P.W. wrote the paper.

This work was supported by the National Institute of Mental Health Grant R33MH104188 (to J.E. and P.W.) and by a German Research Foundation (DFG) award (A.T.).

**Acknowledgments:** We thank Adam Christensen and the University of Oregon Aquatic Care Services staff for excellent zebrafish husbandry. We also thank the University of Oregon Histology Facility for sectioning services and Joseph Bruckner for feedback on drafts of this manuscript.

Correspondence should be addressed to Philip Washbourne at [pwash@uoregon.edu](mailto:pwash@uoregon.edu).

<https://doi.org/10.1523/ENEURO.0035-22.2022>

Copyright © 2022 Tallafuss et al.

This is an open-access article distributed under the terms of the Creative Commons Attribution 4.0 International license, which permits unrestricted use, distribution and reproduction in any medium provided that the original work is properly attributed.

whether *egr1* plays a role in regulating social behavior in this system using established assays, including a high-throughput virtual biological motion assay (Larsch and Baier, 2018). We find that loss of *egr1* function compromises zebrafish social behavior, but not other behaviors. BF *th* expression is also reduced in *egr1* mutants, with a ~30% reduction in TH-positive anterior parvocellular pre-optic nucleus (PPa) neurons. Chemogenetic ablation of about one third of the identified PPa neurons resulted in social behavior deficits, similar to the reduction observed in *egr1* mutants. Our results suggest that *egr1* is required for expression of *th* in a BF population of dopaminergic neurons necessary for normal social interactions, thereby expanding our understanding of the precise circuitry for social behavior.

## Materials and Methods

### Zebrafish husbandry

All zebrafish embryos, larvae, and adults were raised and maintained at 28.5°C according to standard protocols with a 14/10 h light/dark cycle (Westerfield, 2007). Lines used were AB/Tübingen, *egr1<sup>sa64</sup>*, *Et<sup>y321</sup>* [*Et (rex2-scp1:gal4ff)y321*], *Et<sup>y405</sup>* [*Et(scp1:gal4ff)y405*], and *c264Tg(14xuas:nfsB-mCherry)*. The *egr1<sup>sa64</sup>* line, which was generated by ENU mutagenesis during the Sanger Zebrafish Mutation Project (ZMP), was outcrossed to AB/Tübingen for 7 generations before the analysis described. Genotyping was performed for the *egr1<sup>sa64</sup>* allele using a Competitive Allele-Specific PCR SNP genotyping system (KASP, LGC Biosearch Technologies) according to manufacturer's protocols after behavioral assays and before processing for Western blotting and immunolabeling. Animals with unknown genotypes were excluded from experiments and analysis.

### Behavioral assays

#### Split dyad analysis

Socially-motivated place preference and visually-evoked orienting behavior of 14 d postfertilization (dpf) zebrafish were measured using a split dyad assay (Stednitz and Washbourne, 2020). Roughly size-matched larvae from an incross of *egr1<sup>sa64</sup>* heterozygotes (hets) were placed in paired, isolated tanks (50 mm in length × 20 mm in width × 20 mm in depth) separated by an opaque divider and allowed to habituate for 5 min, then the divider was removed and the animals allowed to interact for an additional 5 min. Both the presocial and social stimulus periods were recorded to determine the baseline exploratory and locomotor behavior. Recordings were obtained from below at 10 fps using a Mightex SME-B050-U camera and illuminated by an overhead white LED panel (Environmental Lights). For numbers of animals and their genotypes see Table 1.

#### Biological motion social assays

To explore social engagement, we tested social approach using a virtual social assay that is based on detection of biological motion (Larsch and Baier, 2018). The stimuli, which are dots projected below dishes of solitary animals, are followed when they move in bouts with

**Table 1: Animal numbers and genotypes for behavioral experiments**

Test	Age (dpf)	Total	+/+	+/-	-/-
Split dyad	14	56	9	36	11
Virtual social	14	75	27	36	12
Virtual social	16	129	38	71	20
Virtual social	18	97	30	49	18
Virtual social (pooled)	14/16	201	172	29	
Predator avoidance	14	126	28	77	21

kinetics similar to age matched animals. These assays were performed as described by Larsch and Baier (Larsch and Baier, 2018). Briefly, larvae from an incross of *egr1<sup>sa64</sup>* hets were placed individually in watch glasses filled with facility water. The watch glasses were located in a shallow aquarium on translucent sheets, with a cold mirror and IR LEDs below. A projector, located to the side, projected images onto the translucent sheets by way of the cold mirror. A digital camera with an IR filter was located above the watch glasses. Projector and camera were controlled by bespoke software in Bonsai. Dots of varying sizes were projected intermittently, moving in a synthetic knot shape for a 5-min period. Fish were maintained for 2–3 h in the watch glasses. At each frame, animal and stimulus parameters were streamed to a text file for offline analysis. Fish were tested in facility water at room temperature (25°C). For numbers of animals and their genotypes see Table 1. The numbers for the thigmotaxis and speed analyses are the same as for virtual social at 14 dpf.

#### Chemogenetic ablation experiments

Fourteen days postfertilization larvae from a cross between [*c264Tg(14xuas:nfsB-mCherry)*] and [*Et(scp1:gal4ff)y405*] fish were incubated in the dark for two nights in static facility water with 2.5 μM nifurpirinol (Furanol, JBL), a nitroaromatic antibiotic that is converted into a toxic metabolite by the enzyme nitroreductase. Water flow was restored and larvae were fed during the day. As a control, sibling larvae only expressing GFP, and not the nitroreductase transgene, under the influence of the *Et<sup>y405</sup>* enhancer trap, were analyzed in parallel. Water flow was restored for a minimum of 1 h before biological motion social assays. A total of 60 animals were tested from two experiments with 28 animals expressing GFP only and 32 animals expressing both GFP and nitroreductase.

#### Predator avoidance tests

Predator avoidance was assessed by measuring visually induced escape responses on presentation of looming stimuli as described previously (Fernandes et al., 2021). Briefly, expanding black dots were projected from below to free-swimming animals using custom scripts in Bonsai to control OpenGL drawing routines. Dots were positioned 10 mm left or right with respect to the center of mass and orientation of each animal at the onset of dot expansion. Dots expanded for 500 ms (15 frames) with a linear increase in diameter to their final size ranging from 0 to 12 mm. Looming stimuli of different sizes were presented left or right of the animals once per minute in random order. A moving grating was presented for 20 s

**Table 2: Antibody resources for Western blotting**

Target	Manufacturer	Catalog #, clone	Dilution	Species	Immunogen	RRID
Syn1/2	Synaptic Systems	106002	1:1000	Rb	Rat peptide, aa 2–28	AB_2619773
TH	Millipore Sigma	AB152	1:5000	Rb	Denatured purified protein from rat	AB_390204
$\beta$ -Actin	Santa Cruz	Sc-47778	1:1000	Ms	Purified chicken protein	AB_2714189
pan MAGUK	NeuroMab	K28/86	1:1000	Ms	Human PSD-95 fusion protein (77–289)	AB_2877192

Rb, rabbit; Ms, mouse.

ending 10 s before the presentation of the next loom stimulus to drive larvae toward the center of a dish. At each frame, animal and stimulus parameters were streamed to a text file for offline analysis. Fish were tested at 14 dpf in facility water at room temperature (25°C) for a total of 1 h. For numbers of animals and their genotypes see Table 1.

### ***In situ* hybridization (ISH)**

RNA ISH was conducted on brain cryostat sections (16  $\mu$ m) according to standard protocols (Westerfield, 2007) and using the manufacturer recommended protocols for RNAScope (ACD).

### **Western blotting**

Heads were removed by cutting across the trunk at the level of the heart of anesthetized 15 dpf larvae. Heads were homogenized in RIPA buffer, with the protease inhibitors TLCK, PMSF, and pepstatin. Homogenates were incubated under constant motion at 4°C for 1 h before centrifuging at 12,300  $\times g$  for 20 min at 4°C. The supernatant was removed and the pellet was resuspended in Laemmli sample buffer with 5%  $\beta$ -mercaptoethanol. Samples were heated at 95°C for 5 min, electrophoresed and blotted to nitrocellulose membranes under standard conditions. Antibodies used are listed in Table 2. Secondary antibodies made in donkey and conjugated to IR dyes 680RD and 800CW (LiCor) were revealed with a LiCor Odyssey.

### **Immunolabeling**

Immunolabeling of synaptic markers was performed on brain cryostat sections (16  $\mu$ m) according to standard protocols (Westerfield, 2007). Antibodies used were to Synapsin 1/2 and Gephyrin (Table 3). Immunolabeling of TH and GFP (Table 3) were performed on paraformaldehyde fixed, dissected heads with jaws and dura removed. Permeabilization, blocking and antibody incubations were performed as described previously (Goode et al., 2020). Primary antibodies were revealed using the following secondary antibodies at a concentration of 1:750: Alexa Fluor

goat anti-mouse and rabbit IgG1, IgG<sub>2a</sub>, and (H + L), ThermoFisherScientific, coupled to 488, 546, or 633. Images were taken on a Leica SP8 confocal microscope with LasX software with 10 $\times$ , 20 $\times$ , or 63 $\times$  oil immersion objectives.

### **Quantification and statistics**

#### *Size comparisons*

Animals were considered “stunted” when they were shorter than a threshold set at 1.5 $\times$  the SD below average wild-type (wt) size, measured from tip of nose to the end of the trunk (excluding the tail fin). We measured and genotyped 30–32 randomly selected individuals from 8 clutches for the analysis in Figure 1.

#### *Split dyad analysis*

The percentage of time in motion was calculated as the number of frames in which the animal moved at least one-third of their total body length per frame. Larvae that spent <10% of the experiment in motion were excluded from subsequent analyses. Larvae were genotyped following the experiment as previously described. In separate analyses, data for wt and het animals was pooled and the genotype of the respective stimulus fish was used as the classifier (Fig. 2E,F). Social interaction is parameterized as the average relative distance from the divider (relative place preference) and the percentage of time spent at 45–90° (% time orienting) using previously described software written in Python (Stednitz et al., 2018). Place preference was calculated as the average relative proximity to the divider across all frames. Behavior was compared statistically using a mixed-model repeated measures ANOVA (mmANOVA) in Python, using genotype as the between-subjects factor and time (presocial and during social stimulus) for each metric as the within-subjects factor.

#### *Biological motion social assay and predator avoidance test analysis*

Background subtracted, inverted and thresholded avi files were analyzed using scripts in Jupyter as described

**Table 3: Antibody resources for immunolabeling**

Target	Manufacturer	Catalog #, clone	Dilution	Species	Immunogen	RRID
Syn1/2	Synaptic Systems	106002	1:250	Rb	Rat peptide, aa 2-28	AB_2619773
Gephyrin	Abcam	Ab32206	1:1000	Rb	Ms Peptide, aa 700-C-term	AB_2112628
TH	Millipore Sigma	AB152	1:500	Rb	Denatured purified protein from rat	AB_390204
GFP	Invitrogen	3E6	1:500	Ms	Recombinant GFP	AB_2313858

Rb, rabbit; Ms, mouse.



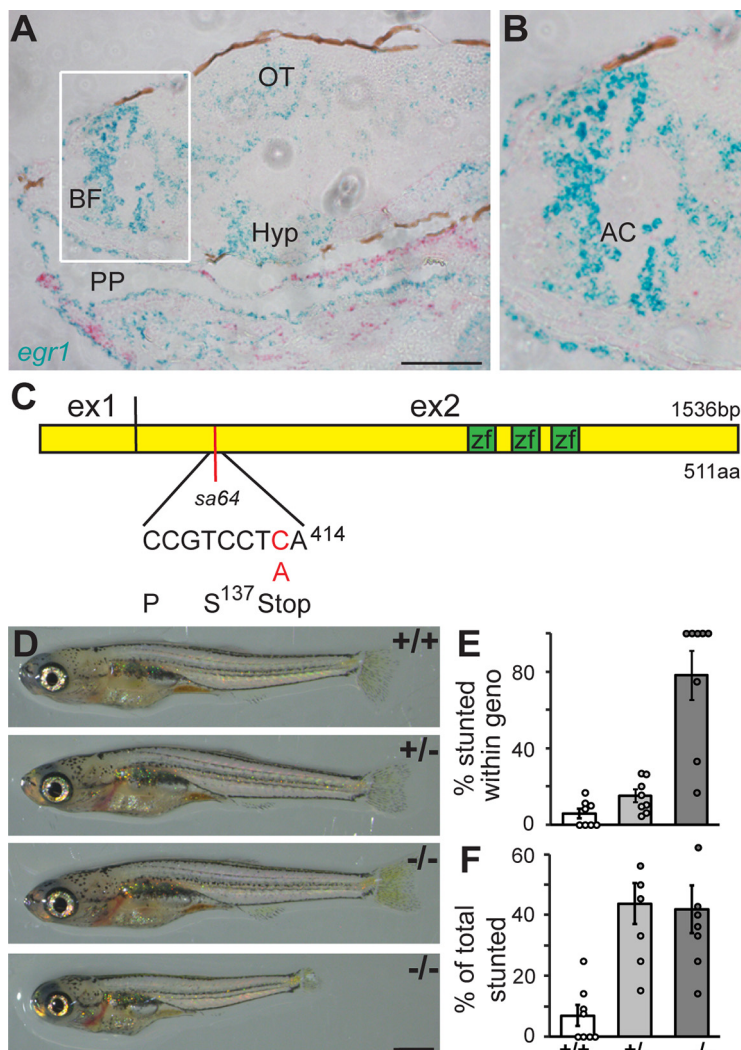


**Figure 1.** *egr1* is expressed in the forebrain. **A**, ISH reveals *egr1* expression (blue) in the basal forebrain (BF), optic tectum (OT), hypothalamus (Hyp), and epithelial cells of the pharyngeal pouch (PP) at 6 dpf. *myogenin d* was used as a control probe (red). Anterior to the left. Scale bar: 100  $\mu$ m. **B**, Magnification of the BF (white box in **A**) showing expression surrounding the anterior commissure (AC). **C**, Exon organization of the *egr1* mRNA, location of the zinc finger domains (zf), and location of the *sa64* mutation (red bar). **D**, *egr1*<sup>sa64</sup> mutants (–/–) develop a normal body plan with functional swim bladder, but with size deficits (bottom). **E**, Close to 80% of mutant larvae are stunted (dark gray). **F**, More than 50% of stunted larvae are also wt (+/+, white) and het animals (+/–, light gray). *N* = 8 clutches, *n* = 248 animals.

previously (Larsch and Baier, 2018). The social index (SI) quantifies attraction of the animal toward the biological motion dot stimulus. SI relates the observed animal-dot distance relative to a predicted distance that would result purely from chance encounters with the stimulus. SI was quantified as previously described (Larsch and Baier, 2018) using python scripts: the “real” observed animal-dot distance was calculated for each animal as an average in 5-min chunks (IADr). Next, we shifted the animal trajectories in time relative to the stimulus trajectory by 10 different offsets >60 s and re-calculated a “shifted” animal-dot distance (IADs) for each time shift. Because of the time shift, IADs reflects the dot-animal distance expected by chance encounters. Mean IADs (mIADs) for all time shifts was used to compute SI as (mIADs-IADr)/mIADs. Significance was determined using JMP software.

A Tukey–Kramer HSD for pairwise comparisons of least square means was applied to the three genotypes with a *p* threshold of 0.05. Data from within the biological motion social assay was also analyzed for motion and thigmotaxis, as described previously (Larsch and Baier, 2018), and significance was determined using HSD.

#### Western blotting

Images of Western blottings were analyzed using LiCor Image Studio software. We only used intensity data for bands that were within the linear range, i.e., not saturated. Total intensity of bands was divided by the total intensity of in-lane  $\beta$ -actin bands. Resulting intensity ratios were then normalized to the mean of wt larvae. A minimum of two technical replicates were analyzed for four biological replicates. Pools of homogenized heads were of a

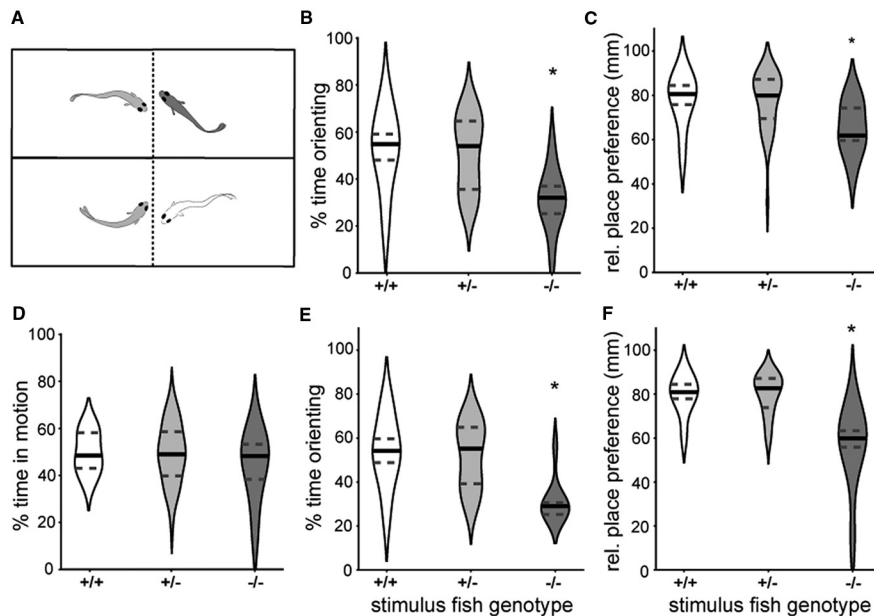


**Figure 2.** *egr1* mutants are less social than wt larvae. **A**, Larvae from an incross of *egr1*<sup>sa64</sup> were placed in roughly size-matched split dyads at 14 dpf and tested for social orienting and place preference, with the ability to see a sibling through glass. Genotypes [wt (white), het (gray), mut (dark gray)] were determined after testing. **B**, *egr1* mutants spent less time orienting at angles between 45° and 90° to the divider.  $n = 56$  animals,  $*p < 0.001$  (mmANOVA). **C**, Relative place preference, as measured from the wall opposite the divider and normalized to the total length, revealed less social engagement for *egr1* mutants. Zero denotes distance furthest from the divider.  $*p < 0.05$  (HSD). **D**, There was no difference in overall activity measured as percent time in motion. Time orienting at angles between 45° and 90° (**E**) and relative place preference (**F**) for het and wt larvae based on the genotype of the stimulus larvae (stimulus fish genotype) revealed that a deficit in the mutants is detected by the het and wt larvae;  $*p < 0.001$  (mmANOVA). Solid black line represents the median, dotted gray lines represent the upper and lower quartiles.

minimum of ten heads of each genotype. Significance was determined using JMP software. HSD for pairwise comparisons of least square means was applied to the three genotypes with a  $p$  threshold of 0.05.

### Synaptic puncta

Cropped sections of 63× images were analyzed in ImageJ using the PunctaAnalyzer plug-in for a region of 77  $\mu\text{m}^2$ . A minimum of eight images for each genotype was quantified. HSD was applied to the analysis of puncta numbers with a  $p$  threshold of 0.05.

## Results

### Egr1 influences overall growth but not development

To identify a role for the *egr1* gene in social behavior, we first examined the expression pattern of *egr1* in developing zebrafish larvae by RNAscope ISH at 6 dpf. This developmental period, during which synaptic circuitry remains dynamic (Goode et al., 2020), occurs one week before the appearance of robust social behavior (Dreosti et al., 2015; Larsch and Baier, 2018; Stednitz and Washbourne, 2020). *egr1*, in addition to being expressed in the pharyngeal pouch (PP; Fig. 1A), is predominantly expressed in a few clusters in the forebrain and midbrain. Given previous evidence for telencephalic contribution to social behavior (Stednitz et al., 2018), we noticed the prominent *egr1* expression in the telencephalon, including the BF, in cells adjoining the anterior commissure (AC;

Fig. 1B). We conclude that *egr1* is expressed in a region that contributes to social behavior at a time when neuronal circuits are being established.

We obtained a mutant from the Sanger ZMP with a point mutation in the *egr1* gene (*sa64*). The C > A mutation generates a premature termination codon in exon 2, likely resulting in a truncated 137-aa protein. As this mutation is located upstream of the functional zinc finger DNA binding motifs (Fig. 1C), we predict that it results in loss of protein function. To eliminate possible additional background mutations, we used *egr1*<sup>sa64</sup> hets that had been outcrossed to wt zebrafish for seven generations.

Larvae derived from an incross of *egr1*<sup>sa64</sup> hets develop normally (Fig. 1D) and homozygous mutants were present at an approximate Mendelian ratio at 15 dpf ( $27.7 \pm 13.6\%$  SD;  $N = 4$  clutches,  $n = 201$  animals), a developmental time at which social behavior is already robust (Stednitz and Washbourne, 2020). However, we noticed a large proportion of larvae that were much smaller ( $<$  the mean minus  $1.5 \times$  the SD) than others, which we will call “stunted.” Mutants were significantly smaller than wt and hets on average ( $p = 0.002$ ,  $p = 0.006$ ), although stunted individuals were found across all genotypes and reached other developmental milestones with their siblings (Fig. 1D, bottom). For example, stunted larvae inflated their swim bladders by the same day (5 dpf) as all other animals, including homozygous *egr1*<sup>sa64</sup> mutants. Although the majority of homozygous *egr1* mutants were stunted ( $78 \pm 12.9\%$  SE across 8 clutches; Fig. 1E), almost half of

the stunted larvae occurred in het and wt larvae (Fig. 1F). This phenotype is similar to the stunted growth reported in the mouse *Egr1* gene knock-out mutant (Topilko et al., 1998). Analysis of *egr1* using morpholine-modified oligonucleotides (MO) in zebrafish also resulted in reduced growth in morphants (Zhang et al., 2013). Therefore, despite the incomplete penetrance in our system, we conclude that *egr1* contributes to size of the animal. Because of the relatively high occurrence of the stunted phenotype in hets, we conclude that this phenotype may be because of a gene interaction with an, as yet, undetermined other gene. We also conclude that *egr1<sup>sa64</sup>* is likely to be a null allele, although we cannot exclude the possibility that it is a hypomorph. Importantly, we considered size as a factor for all additional experiments.

### Egr1 is necessary for social behavior

To examine social behavior in *egr1<sup>sa64</sup>* mutants of regular-sized and stunted animals, we used a split dyad assay with size-matched animals (Fig. 2A; Stednitz et al., 2018). Social behavior becomes robust at 14 dpf and is visually driven, with animals engaging in stereotypical orienting and approach behavior when they can see an animal of similar size (Dreosti et al., 2015; Stednitz and Washbourne, 2020). *egr1* mutants spent less time orienting at angles to the divider between 45° and 90° ( $p = 0.003$ ; Fig. 2B), a strong indicator of social engagement (Stednitz et al., 2018), and less time close to the divider (Fig. 2C). Mutants were not less active during the assay period ( $p = 0.131$ ; Fig. 2D). We conclude that Egr1 is involved in modulating social behavior.

Consistent with our previous findings on active reciprocity during social interactions in adult and larval zebrafish, wt and heterozygous fish paired with mutants also exhibited reduced social orienting ( $p = 0.003$ ; Fig. 2E) and place preference ( $p < 0.001$ ; Fig. 2F). Using multiple linear regression, we found that both the genotype of the target fish and the stimulus fish significantly influences orienting behavior ( $p = 0.021$  and  $p = 0.040$ , respectively). Therefore, the deficit in social behavior of *egr1* mutants is detected by wt and heterozygous siblings. However, we also conclude that this social assay provides a variable social stimulus for test larvae that might lead to spurious results, especially with the added size effect.

To explore social engagement without stimulus variability, we tested whether a social deficit could also be detected using a virtual social assay that is based on detection of biological motion (Larsch and Baier, 2018). This assay reduces variability, as the stimulus is identical for each larva. Dots projected below dishes of solitary animals are followed preferentially when the dots move in bouts with kinetics similar to age matched animals (Fig. 3A; Larsch and Baier, 2018). Animal responses are tuned to dot size, with maximal social attraction at dot sizes approximating body size at 4.0 mm for 14 dpf larvae (Fig. 3B; Larsch and Baier, 2018). Larger dots (16 mm) elicit an aversive response, whereas small dots (0.5 mm) are ignored and are equivalent to no dot (0.0; Fig. 3B). Homozygous *egr1<sup>sa64</sup>* mutant larvae are less attracted to visual stimuli 2.0, 4.0, and 8.0 mm in diameter than wt

siblings ( $p = 0.0086, 0.0034, 0.047$ , HSD; Fig. 3B). This reduction in social behavior is also evident at 16 and 18 dpf ( $p < 0.0001, p = 0.009$ , HSD), suggesting the deficit is not a short developmental delay that is recuperated over 4 d of development (Fig. 3C). *egr1* genotype does not affect animal swimming speed or thigmotaxis ( $p = 0.69, 0.76$ , HSD; Fig. 3D,E). Furthermore, predator avoidance responses to a looming stimulus are not significantly different between all genotypes at 14 dpf ( $p > 0.25$ ; HSD; Fig. 3F), suggesting that vision is not accountable for the reduction in SI. We conclude that Egr1 is necessary for following biological motion in a social context, but not for visual and motor system functions.

We considered that the growth deficit (Fig. 1D–F) might account for the reduction in SI. We detected a weak, yet significant, correlation between animal size and SI ( $R = 0.37, R^2 = 0.14, p = 0.0011$ ; Fig. 3G). This effect was consistent across individual genotypes and at all ages examined. We further explored the influence of size by comparing the SI of animals in groups of similar size. Consistent with previous observations (Larsch and Baier, 2018), larger wt and heterozygote animals have a 67% higher SI than wt stunted animals ( $p = 0.186$ , HSD,  $n = 9$  stunted animals; Fig. 3H, +). However, mutants exhibited reduced social behavior both for regular-sized and stunted individuals ( $p = 0.0001$ , HSD; Fig. 3H, –/–). We conclude that genotype, rather than size, is the primary factor influencing social behavior deficits in *egr1* mutants.

### Egr1 is necessary for TH2 expression

The Egr1 transcription factor regulates expression of proteins that play a role in synaptic transmission and NT synthesis (Duclot and Kabbaj, 2017). We used Western blotting of protein extracts from 15 dpf larval heads to explore whether Egr1 promotes social behavior by influencing abundance of such proteins in the brain. Levels of MAGUK proteins (panMAGUK), such as PSD-95, SAP102 and SAP97, and Synapsin proteins 1 and 2 (Synapsin 1/2) were not significantly influenced by *egr1* loss of function ( $p > 0.8$ , HSD; Fig. 4A–C). In contrast, an antibody that recognizes two forms of TH, which based on predicted molecular weights likely correspond to TH1 and TH2, revealed that levels of TH2 but not TH1 are compromised by mutation in *egr1* (TH1:  $p = 0.9$ , TH2:  $p = 0.0485$ , HSD; Fig. 4A,A',D,E).

Given the bias of Egr1 toward regulating synaptic genes (Duclot and Kabbaj, 2017), we assessed whether Egr1 influences forebrain synapse abundance. We quantified synapses by immunolabeling sections of 15 dpf larval brains with antibodies to Synapsin 1/2 and Gephyrin in *egr1<sup>sa64</sup>* mutants (Fig. 4F). Synapsins are enriched at over 95% of vertebrate synapses (Micheva et al., 2010), whereas Gephyrin is a specific marker of inhibitory synapses (Fritschy et al., 2008). Within the BF, a region with high expression of *egr1* (Fig. 1A,B) and a region implicated in controlling social behavior (Stednitz et al., 2018), we focused on the neuropil of the AC. Quantification of the number of puncta, an approximation of synapses, in the medial and lateral AC neuropil showed no difference in



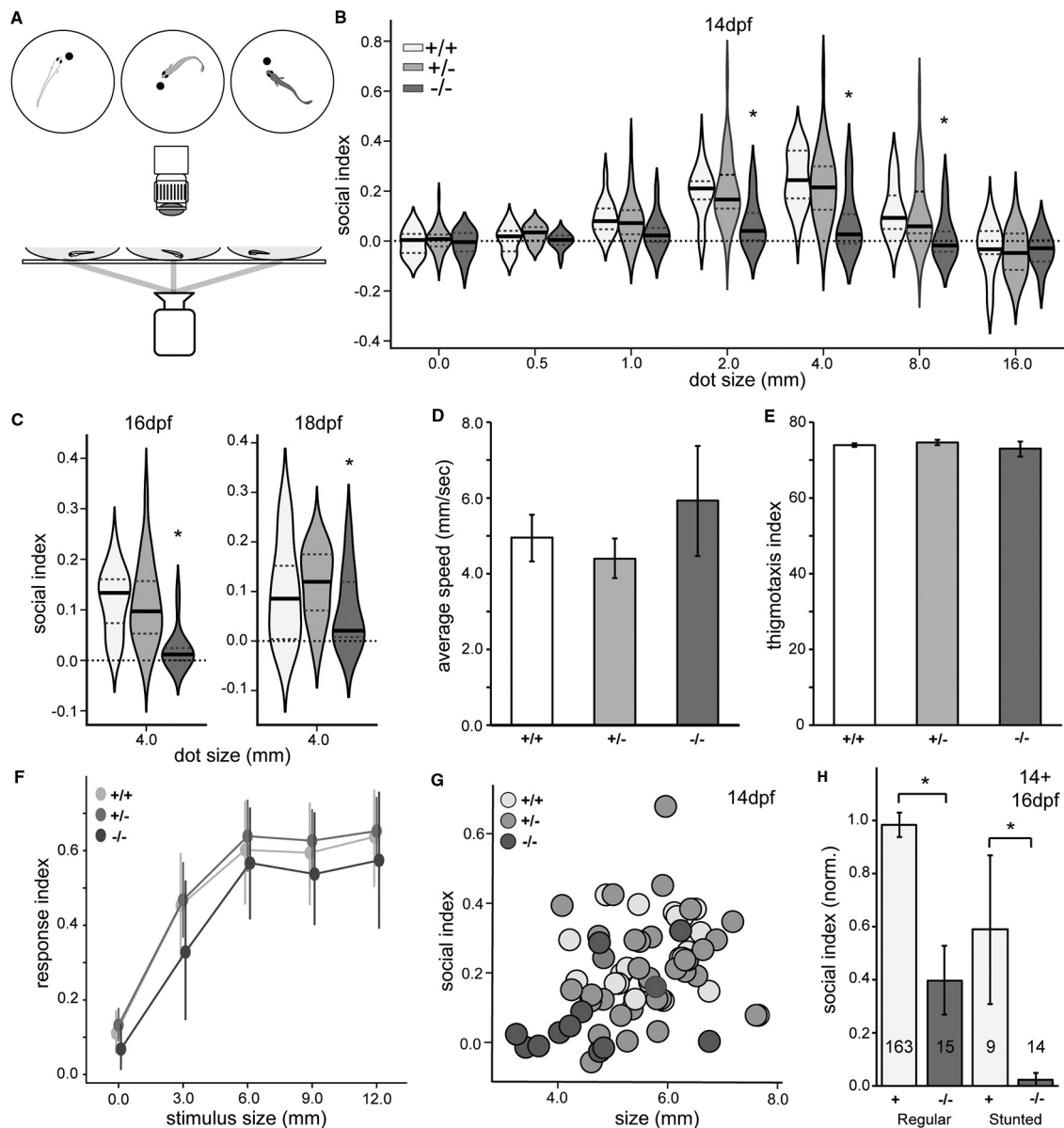


**Figure 3.** *egr1* mutants are less social with virtual stimuli than wt larvae. **A**, Biological motion-based social behavior was assayed by projecting dots of different sizes to dishes from below, while recording with an IR camera from above. **B**, Violin plots revealed significant differences for *egr1* mutants in SI for dot sizes of 2.0, 4.0, and 8.0 mm at 14 dpf.  $N=3$  experiments,  $n=75$  animals  $*p < 0.05$ , HSD, wt (+/+, white), het (+/-, light gray), mut (-/-, dark gray). **C**, *egr1* mutants exhibited social deficits at 16 and 18 dpf, shown for optimal dot size 4.0 mm (dot size with highest SI response).  $N=3$  experiments,  $n=129$  animals, and  $N=3$  experiments,  $n=97$  animals,  $*p < 0.05$ , HSD. Plots of average speed in pixels per second (**D**) and thigmotaxis index (**E**) during biological-motion based assays at 4.0 mm dot size revealed no general behavioral deficits for *egr1* mutants.  $N=3$  experiments,  $n=77$  animals. **F**, Mutant predator avoidance responses were not significantly different from het and wt siblings across various stimulus sizes at 14 dpf.  $N=3$  experiments,  $n=126$  animals. **G**, Correlation plot of size (in pixels) and SI for 4 mm dot size at 14 dpf.  $N=3$  experiments,  $n=75$  animals. **H**, The differences in SI for 4.0 mm dot size in 14 and 16 dpf larvae (normalized to average 14 dpf wt SI) between mutants and wt/hets (+, white) are significant in both regular-sized and stunted larvae.  $n=201$  animals,  $*p < 0.05$ , HSD. Error bars are SEM. Animal numbers are presented on bars.

total (Synapsin 1/2,  $p=0.71$ , HSD) or inhibitory (Gephyrin,  $p=0.99$ , HSD) puncta density in *egr1* mutants compared with wt (Fig. 4G). The lack of effect on synapse number is consistent with the Western blotting results above, which demonstrated that levels of the widespread synapse markers Synapsin 1/2 and PSD-95 are unchanged in *egr1*

mutants. However, our results do not preclude the possibility that specific synapse populations might be regulated by Egr1. We conclude that Egr1 regulates the abundance of TH2 protein, but does not regulate presynaptic or postsynaptic protein abundance of Synapsin 1/2 or MAGUK proteins, nor general synapse density.



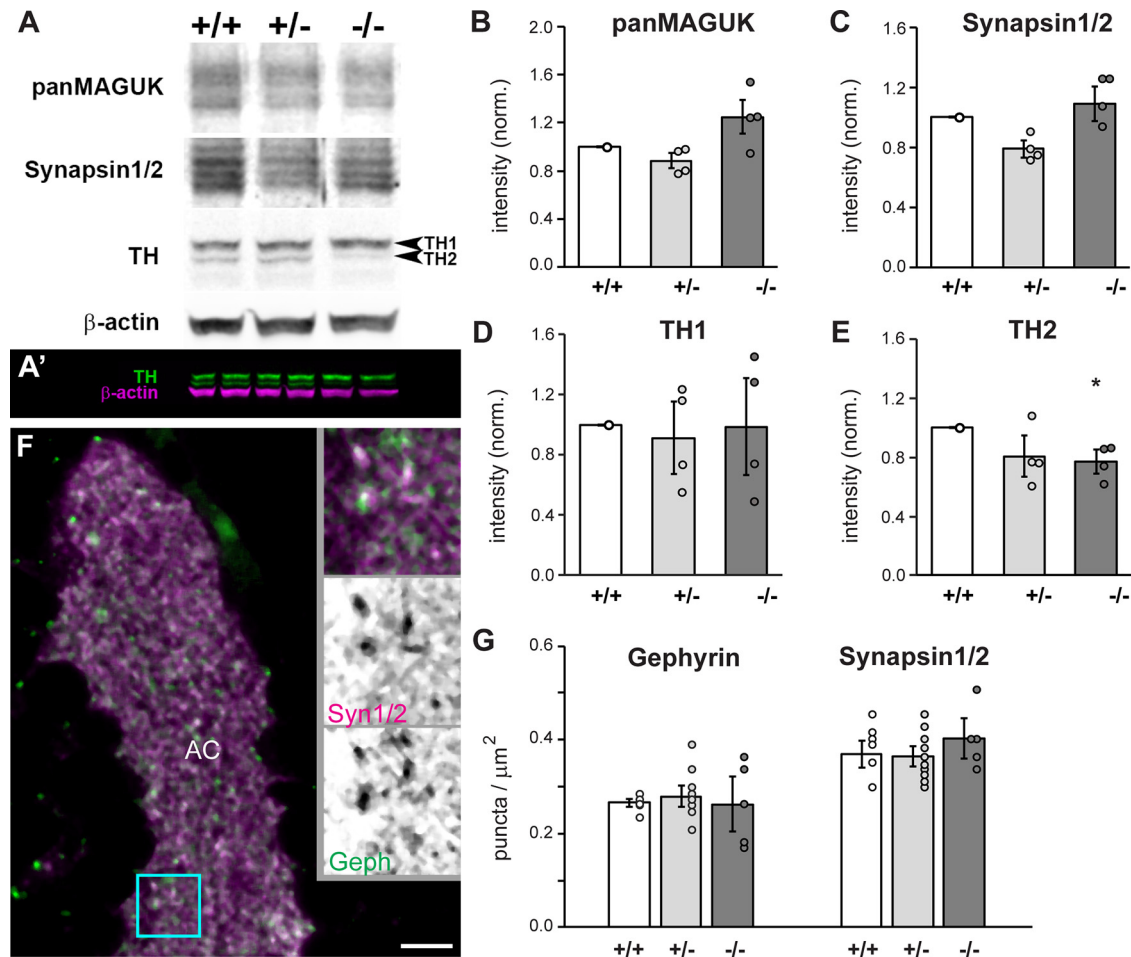


**Figure 4.** *Egr1* is necessary for TH2 expression. **A**, Western blotting of larval head homogenates at 14 dpf reveals a reduction in expression of TH2 in *egr1* mutants. **A'**, Two color labeling of a Western blotting to highlight in-lane normalization to  $\beta$ -actin and technical replicates. **B–E**, Western blot intensities in **A**, **A'** were first normalized to in-lane  $\beta$ -actin, and then to wt average intensity.  $N=4$  experiments,  $n=2$  technical replicates,  $*p < 0.05$ , HSD. **F**, Immunolabeling of synapses with antibodies to Synapsin 1 and 2 (Syn1/2, magenta) and Gephyrin (Geph, green) in the anterior commissure (AC), lateral view. Insets are magnifications of the cyan box. Scale bar:  $5\ \mu\text{m}$ . **G**, Quantification of synaptic puncta revealed no changes in synapse density in the medial and lateral AC.  $n \geq 5$  brains per genotype. wt (+/+, white), het (+/-, light gray), mut (-/-, dark gray). Error bars are SEM.

A synaptic connection between TH-positive neurons and cholinergic BF neurons (cBFNs) defined by the enhancer trap line *Et<sup>y321</sup> [Et(rex2-scp1:gal4ff)y321]* was recently identified (Goode et al., 2020). Chemogenetic ablation of cBFNs disrupts social attraction and orienting behavior (Stednitz et al., 2018). Images from the most basal region of the forebrain (Fig. 5E), including the anterior part of the presumptive PPA, reveal that the TH-positive neurons project to the AC neuropil (Fig. 5A–A'', white arrows), which is also innervated by cBFN arbors (Goode et al., 2020). TH-positive neurons in the PPA are highly likely to be dopaminergic (Yamamoto et al., 2011), so we will refer to these cells as dPPaNs. Cells in this region have been documented to express both *th1* and *th2* genes in larvae and adults (Semenova et al., 2014).

We explored whether TH expression in dPPaNs requires *Egr1* (Fig. 5B–D). The number of TH-positive dPPaNs was significantly reduced in homozygous *egr1<sup>sa64</sup>* mutants relative to wt siblings at 14 dpf

( $p = 0.049$ , HSD; Fig. 5F). The  $\sim 28\%$  reduction of TH-positive dPPaNs in mutants was evident as early as 7 dpf (Fig. 5G), a time at which stunted individuals were not detected. Interestingly, we found an intermediate, but not significant, phenotype in TH cell number in heterozygous *egr1<sup>sa64</sup>* mutants as compared with wts at both time points ( $p = 0.362$ ,  $p = 0.099$ , HSD), analogous to results from the Western blot experiments (Fig. 4E). This may indicate a haplo-insufficiency at the molecular level, although this is not detected at the behavioral level. Together, our results suggest that the discrepancy in TH expressing cells is established early in development, consistent with the expression of *egr1* in the BF at this developmental stage (Fig. 1B). Given the expression of both *th1* and *th2* in dPPaNs (Semenova et al., 2014), we conclude that our result is because of a decrease in the actual number of dPPaNs, and not because of a detection limit as a consequence of a *th2* expression decrease. Our experiments suggest that

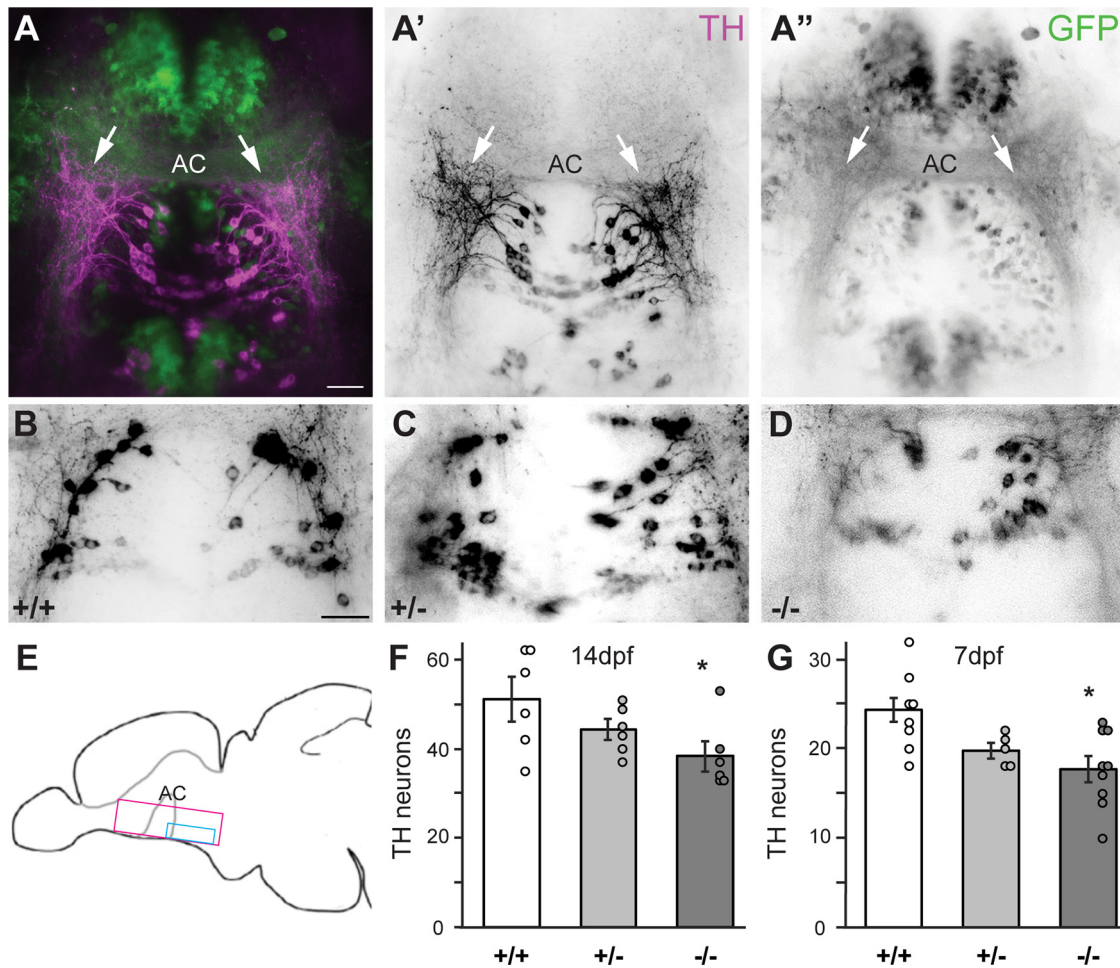


**Figure 5.** *Egr1* is necessary for TH-positive neuron number in BF. **A–A''**, Dorsal view of maximum projection of the BF region (magenta box in **E**) of *Et<sup>y321</sup>* larval zebrafish at 14 dpf labeled with antibodies to GFP (green) and TH (magenta). Anterior commissure (AC); anterior is to the top. **B–D**, Maximum projections of TH labeling in the BF region posterior to the AC for *egr1* wt (**B**), hets (**C**) and mutants (**D**). Scale bars: 30  $\mu$ m. **E**, Diagrammatic side-view of the larval brain highlighting the regions (magenta and cyan) analyzed as a maximum projection Z-stacks in **A**, **B–D**, respectively. **F**, Quantification of the number of TH-positive neurons in the cyan region in **E** revealed a decrease in *egr1* mutants at 14 dpf.  $N=2$  experiments,  $n=18$  brains,  $p < 0.05$  (HSD). **G**, The same quantification as in **F** at 7 dpf demonstrates a consistent decrease in TH-positive neurons during development.  $N=2$ ,  $n=24$ ,  $p < 0.05$  (HSD). wt (+/+), white), het (+/-, light gray), mut (-/-, dark gray). Error bars are SEM.

catecholaminergic, presumably dopaminergic, signaling in this part of the larval brain is compromised by loss of *Egr1*, although it is possible that feedback mechanisms might compensate for the NT deficit.

**BF TH neurons are necessary for social behavior**

To gain genetic access to the TH-positive neuron population and test a possible role for these neurons in social behavior, we examined driver lines that express in the BF. The *Tg(galanin:GFP)* line expresses in neurons in the PPa, and the neuropeptide galanin has been implicated in various mammalian social behaviors (Wu et al., 2014). Labeling of *galanin:GFP* transgenic animals with TH antibody revealed that galanin-expressing and TH-positive neurons are distinct populations (Fig. 6A). The enhancer trap line *Et<sup>y405</sup> [Et(scp1:gal4ff)y405]*, in which the construct integrated in the *robo2* gene, also drives expression in the PPa. In contrast to the galanin driver, ~30% of

neurons labeled by the *Et<sup>y405</sup>* driver overlapped with TH-positive dPPaNs ( $29.2 \pm 5.1\%$ ,  $N=3$  brains; Fig. 6B).

We hypothesized that chemogenetic ablation of neurons marked by *Et<sup>y405</sup>* would reduce dPPaNs similar to *egr1* loss of function, allowing us to test whether a reduction of dPPaNs might be the cause of reduced social behavior in *egr1* mutants. We treated larvae generated by a cross between the *Et<sup>y405</sup>* driver and a nitroreductase expression line with the antibiotic nifurpirinol. The enzymatic activity of nitroreductase on nifurpirinol generates a toxic by-product that kills cells in a cell-autonomous fashion. Indeed, treatment of animals with nifurpirinol resulted in a 31% reduction in dPPaNs when the nitroreductase transgene was expressed (GFP control:  $82 \text{ neurons} \pm 2.5$ , nitroreductase:  $56.2 \pm 5$ ,  $n=11$  brains,  $p < 0.005$ , *t* test). Biological motion-based social behavior was significantly reduced in larvae with ablated dPPaNs compared with control animals at dot sizes 2.0, 4.0, 8.0, and 16.0

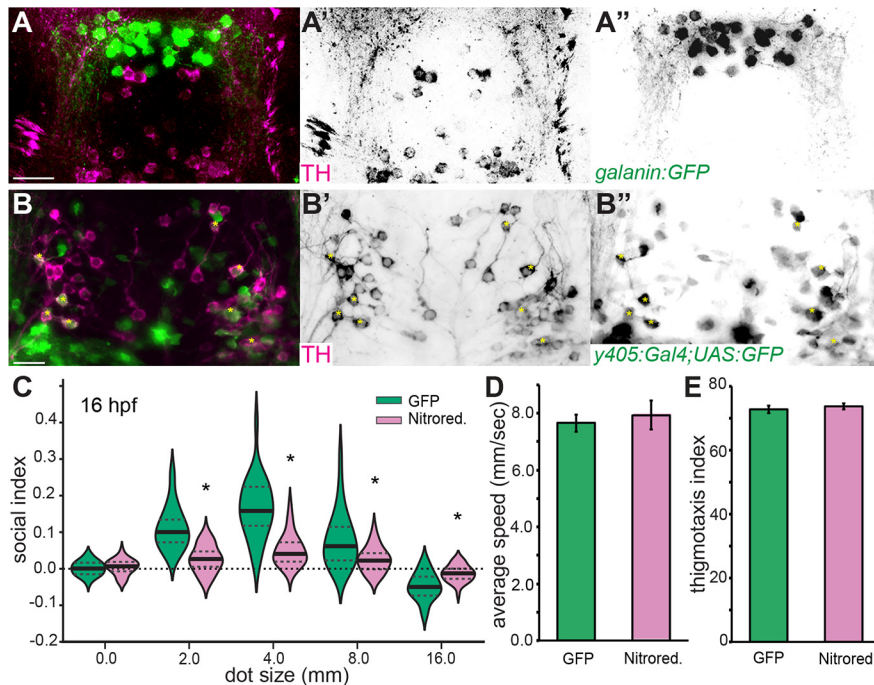


**Figure 6.** TH-positive neurons in PPA are necessary for social behavior. **A–A''**, Maximum projection of the PPA of 14 dpf *Tg(galanin:GFP)* larvae immunolabeled for GFP (green) and TH (magenta) revealed two distinct populations. Dorsal view of cyan box in [Figure 5E](#), anterior to the top. **B–B''**, Maximum projection of PPA of 14 dpf *Et<sup>y405</sup>* larvae immunolabeled for GFP (green) and TH (magenta) revealed transgene expression in ~30% of TH-positive neurons (yellow asterisks). Scale bars: 20  $\mu$ m. **C**, Violin plots of SI for *Et<sup>y405</sup>* larvae with nitroreductase-ablated neurons at 16 dpf (magenta) revealed significant differences compared with control larvae only expressing GFP (green). Both groups were treated with nifurpirinol.  $N=2$  experiments,  $n=60$  animals,  $^*p < 0.001$ ,  $t$  test comparisons to GFP control. Plots of average speed in pixels per second (**D**) and thigmotaxis index (**E**) during biological-motion based assays at 4.0 mm dot size revealed no general behavioral deficits for larvae with *Et<sup>y405</sup>* neurons ablated.  $N=2$  experiments,  $n=60$  animals,  $p > 0.5$ . Error bars are SEM.

( $p < 0.001$ ,  $t$  test; [Fig. 6C](#)). No deficits were detected for swimming speed or thigmotaxis ( $p > 0.5$ ,  $t$  test; [Fig. 6D,E](#)). Chemogenetic ablation of random neuronal populations in larvae does not always cause a deficit in social behavior ([Stednitz et al., 2018](#)), suggesting that the social behavior deficit is specific to the ablated population and not because of general neurologic trauma. We cannot exclude that ablation of neurons in other regions of the brain within the *Et<sup>y405</sup>* line might contribute to the social deficit, as the *Et<sup>y405</sup>* enhancer trap drives sparse expression throughout the brain at 16 dpf ([Fig. 7](#)). However, our results are consistent with the conclusion that dPPaNs are necessary for robust social behavior.

## Discussion

In this study, we examined the contribution of *egr1*, a gene implicated in the etiology of neuropsychiatric disorders, to the establishment of social behavior in zebrafish. *Egr1* regulates social behavior as measured by two different assays: a split dyad assay ([Fig. 2](#)) and a biological motion-based assay ([Fig. 3](#)). Investigation of downstream proteins that might be affected by a loss of this transcription factor revealed a decrease in TH2 protein, but no differences in other known targets of *Egr1* ([Fig. 4](#)). We examined a population of TH-positive neurons in the PPA that are in synaptic contact with identified “social”

neurons of the BF and discovered a reduction in the number of the TH-positive neurons in *egr1* mutants ([Fig. 5](#)). Chemogenetic ablation of a similar number of TH-positive neurons in the PPA resulted in a comparable reduction in social behavior ([Fig. 6](#)).

Our findings using *egr1<sup>sa64</sup>* suggest two important conclusions: (1) *Egr1* is implicated in regulating social behavior, and (2) dPPaNs represent a novel population of neurons implicated in driving social behavior. We discuss these findings further below.

First, the behavioral deficit in *egr1* mutants appears to be relatively specific to social behavior, as it does not affect vision or general motility. This specificity may lie in the *egr1* expression pattern. From the first day of development, *egr1* is specifically expressed in the ventral telencephalon and diencephalon ([Close et al., 2002](#)). This expression is puzzling for an IEG, as it appears long before one would predict high levels of neuronal activity. In fact, activity in the BF social circuit presumably starts during the second week of development, as this is when social behavior becomes apparent ([Stednitz and Washbourne, 2020](#)). Interestingly, *Egr1* has been described to act as a developmental transcription factor in some tissues, for example during development of skeletal muscle ([Zhang et al., 2018](#)). Therefore, it is possible that a primary role of *Egr1* in the BF is activity-independent regulation of TH expression in dPPaNs. In the



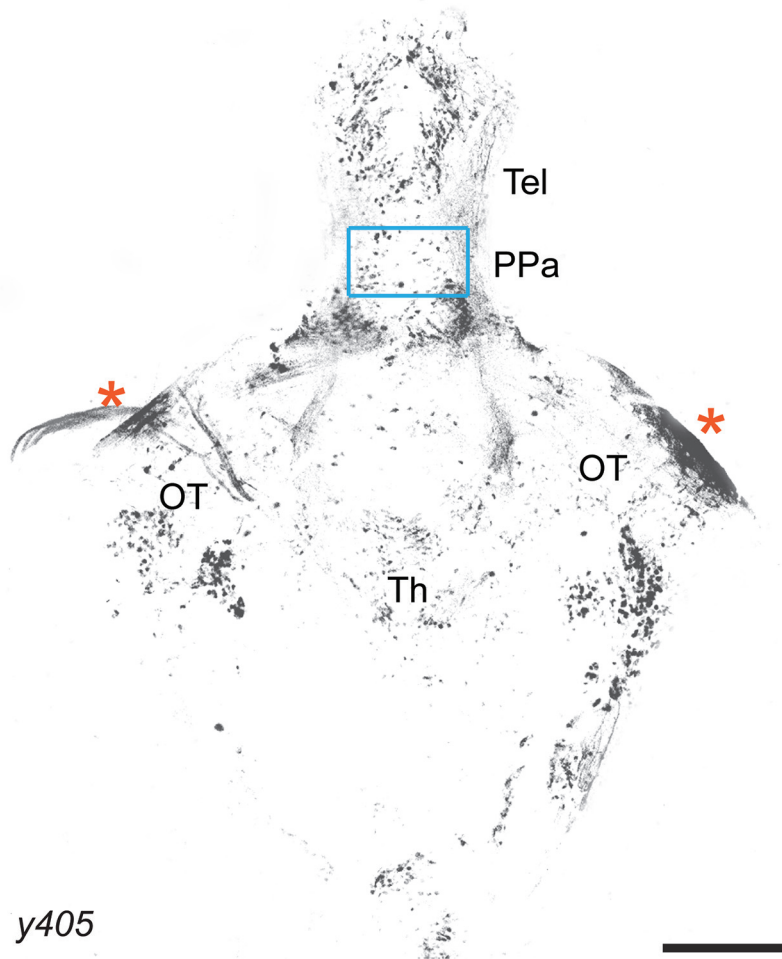


**Figure 7.** Whole-brain expression of *Et y405* at 16 dpf. Maximum Z projection of *Et y405* (*y405*) brain expressing GFP, with the region of interest from [Figure 6B](#) marked with a cyan box. Anterior to the top; \* nonspecific labeling of meninges. Tel, telencephalon; PPa, anterior parvocellular POA; OT, optic tectum; Th, thalamus. Scale bar: 200  $\mu\text{m}$ .

absence of *egr1* expression, dPPaNs presumably synthesize and release less dopamine, reducing critical input to cBFNs and a putative social network in the BF, resulting in aberrant social behavior. Our finding is reminiscent of the loss of another IEG, *FosB*, in mammals. Most behaviors are largely the same in *FosB* knock-out mice, suggesting no ongoing deficit in neuronal function across most of the brain. However, nurturing of neonates is almost absent in knock-out dams, which was explained by deficient signaling in the POA ([Brown et al., 1996](#)). This may suggest an intriguing role for IEGs in establishing circuitry and/or cell type during development, and in the cases of *Egr1* and *FosB*, particularly within social brain networks.

Indeed, the effect we describe in zebrafish induced by the *egr1* mutation is consistent with the identification of *EGR1* as a susceptibility gene for neuropsychiatric disorders including schizophrenia and depression ([Covington et al., 2010](#); [Kimoto et al., 2014](#); [Cattane et al., 2015](#)). Our results also bolster the idea that *EGR1* is a hub for other genes involved in synaptic transmission that are affected in ASD ([Liu et al., 2016](#)). Although *EGR1* levels are altered in various disorders including schizophrenia ([Yamada et](#)

[al., 2007](#)), it is important to note that mutations in the human population have not yet been identified which directly link *EGR1* and these disorders. It is possible that in humans *EGR1* mutations are severe or lethal, and that only other mutations or environmental influences that modulate *EGR1* activity or expression levels result in neuropsychiatric symptoms. This postulated exclusive mode of *EGR1* modulation via other effectors may be unique to humans, as the gene has been implicated in a human-only network of genes aberrant in ASD cases ([Liu et al., 2016](#)).

Second, our study of the molecular mechanisms underlying the social phenotype of *egr1* mutants implicates a population of neurons, dPPaNs, and their connections in driving social behavior. The PPa region lies within the POA, an integral part of the conserved vertebrate social behavior network ([O'Connell and Hofmann, 2012](#)). Consistent with this categorization, the PPa was recently implicated in zebrafish social behavior. Developmental oxytocin-cell ablation, which reduces social behavior, eliminates activation of the PPa by social stimuli ([Nunes et al., 2021](#)). Our results now define a precise population of cells within the PPa that



play a role in controlling social approach and orienting. Our previous finding that TH-positive terminals synapse on cBFN<sup>y321</sup> arbors suggests that the dPPaNs identified here are presynaptic to cBFNs (Goode et al., 2020). It is yet more intriguing to consider that these terminals increase their Synaptotagmin 2a protein levels when social behavior becomes robust at 14 dpf (Goode et al., 2020), implicating a developmental gain of function in the dPPaNs as the trigger that “turns on” social behavior. This insight now ties two concrete neuronal populations together as a first step in elucidating a social circuit at molecular and cellular resolution.

Finally, based on anatomic marker studies of the developing zebrafish brain, the TH-positive PPaNs are most probably dopaminergic (Yamamoto et al., 2011; Gunaydin and Deisseroth, 2014). The putative dopaminergic identity of dPPaNs raises interesting possibilities, as the dopamine system is affected in neuropsychiatric disorders with social components, such as ASD (Hettinger et al., 2008). Dopamine is generally considered to be part of a reward system; therefore, dPPaNs could be part of a reward circuit for social motivation (Gunaydin and Deisseroth, 2014). Alternatively, dPPaNs could also modulate social cognition (Gunaydin and Deisseroth, 2014). Future studies to discriminate between these two options will be critical for understanding the circuits and mechanisms underlying social approach and orienting behavior. Although further transcriptomic characterization will help to define the molecular identity of dPPaNs, our findings already inform potential pharmacological intervention strategies for the social component of neuropsychiatric disorders.

## References

- Anneser L, Alcantara IC, Gemmer A, Mirkes K, Ryu S, Schuman EM (2020) The neuropeptide Pth2 dynamically senses others via mechanosensation. *Nature* 588:653–657.
- Brown JR, Ye H, Bronson RT, Dikkes P, Greenberg ME (1996) A defect in nurturing in mice lacking the immediate early gene fosB. *Cell* 86:297–309.
- Burmeister SS, Jarvis ED, Fernald RD (2005) Rapid behavioral and genomic responses to social opportunity. *PLoS Biol* 3:e363.
- Cattane N, Minelli A, Milanese E, Maj C, Bignotti S, Bortolomasi M, Bocchio Chiavetto L, Gennarelli M (2015) Altered gene expression in schizophrenia: findings from transcriptional signatures in fibroblasts and blood. *PLoS One* 10:e0116686.
- Close R, Toro S, Martial JA, Muller M (2002) Expression of the zinc finger Egr1 gene during zebrafish embryonic development. *Mech Dev* 118:269–272.
- Covington HE 3rd, Lobo MK, Maze I, Vialou V, Hyman JM, Zaman S, LaPlant Q, Mouzon E, Ghose S, Tammimga CA, Neve RL, Deisseroth K, Nestler EJ (2010) Antidepressant effect of optogenetic stimulation of the medial prefrontal cortex. *J Neurosci* 30:16082–16090.
- Czéh B, Fuchs E, Wiborg O, Simon M (2016) Animal models of major depression and their clinical implications. *Prog Neuropsychopharmacol Biol Psychiatry* 64:293–310.
- Dossat AM, Jourdi H, Wright KN, Strong CE, Sarkar A, Kabbaj M (2017) Viral-mediated Zif268 expression in the prefrontal cortex protects against gonadectomy-induced working memory, long-term memory, and social interaction deficits in male rats. *Neuroscience* 340:243–257.
- Dreosti E, Lopes G, Kampff AR, Wilson SW (2015) Development of social behavior in young zebrafish. *Front Neural Circuits* 9:39.
- Duclot F, Kabbaj M (2017) The role of early growth response 1 (EGR1) in brain plasticity and neuropsychiatric disorders. *Front Behav Neurosci* 11:35.
- Fernald RD (2012) Social control of the brain. *Annu Rev Neurosci* 35:133–151.
- Fernandes AM, Mearns DS, Donovan JC, Larsch J, Helmbrecht TO, Kölsch Y, Laurell E, Kawakami K, Dal Maschio M, Baier H (2021) Neural circuitry for stimulus selection in the zebrafish visual system. *Neuron* 109:805–822.e6.
- Fritschy JM, Harvey RJ, Schwarz G (2008) Gephyrin: where do we stand, where do we go? *Trends Neurosci* 31:257–264.
- Goode C, Voehn M, Ncube D, Eisen J, Washbourne P, Tallafuss A (2020) Late onset of Synaptotagmin 2a expression at synapses relevant to social behavior. *J Comp Neurol* 529:2176–2188.
- Gunaydin LA, Deisseroth K (2014) Dopaminergic dynamics contributing to social behavior. *Cold Spring Harb Symp Quant Biol* 79:221–227.
- Hettinger JA, Liu X, Schwartz CE, Michaelis RC, Holden JJ (2008) A DRD1 haplotype is associated with risk for autism spectrum disorders in male-only affected sib-pair families. *Am J Med Genet B Neuropsychiatr Genet* 147B:628–636.
- Kimoto S, Bazmi HH, Lewis DA (2014) Lower expression of glutamic acid decarboxylase 67 in the prefrontal cortex in schizophrenia: contribution of altered regulation by Zif268. *Am J Psychiatry* 171:969–978.
- Kress S, Wullimann MF (2012) Correlated basal expression of immediate early gene *egr1* and tyrosine hydroxylase in zebrafish brain and downregulation in olfactory bulb after transitory olfactory deprivation. *J Chem Neuroanat* 46:51–66.
- Larsch J, Baier H (2018) Biological motion as an innate perceptual mechanism driving social affiliation. *Curr Biol* 28:3523–3532.e4.
- Liu X, Han D, Somel M, Jiang X, Hu H, Guijarro P, Zhang N, Mitchell A, Halene T, Ely JJ, Sherwood CC, Hof PR, Qiu Z, Pääbo S, Akbarian S, Khaitovich P (2016) Disruption of an evolutionarily novel synaptic expression pattern in autism. *PLoS Biol* 14:e1002558.
- Micheva KD, Busse B, Weiler NC, O'Rourke N, Smith SJ (2010) Single-synapse analysis of a diverse synapse population: proteomic imaging methods and markers. *Neuron* 68:639–653.
- Nunes AR, Gliksberg M, Varela SAM, Teles M, Wircer E, Blechman J, Petri G, Levkowitz G, Oliveira RF (2021) Developmental effects of oxytocin neurons on social affiliation and processing of social information. *J Neurosci* 41:8742–8760.
- O'Connell LA, Hofmann HA (2012) Evolution of a vertebrate social decision-making network. *Science* 336:1154–1157.
- Papanikolaou NA, Sabban EL (2000) Ability of Egr1 to activate tyrosine hydroxylase transcription in PC12 cells. Cross-talk with AP-1 factors. *J Biol Chem* 275:26683–26689.
- Qin X, Jiang Y, Tse YC, Wang Y, Wong TP, Paudel HK (2015) Early growth response 1 (Egr-1) regulates *N*-methyl-D-aspartate receptor (NMDAR)-dependent transcription of PSD-95 and  $\alpha$ -amino-3-hydroxy-5-methyl-4-isoxazole propionic acid receptor (AMPA) trafficking in hippocampal primary neurons. *J Biol Chem* 290:29603–29616.
- Semenova SA, Chen YC, Zhao X, Rauvala H, Panula P (2014) The tyrosine hydroxylase 2 (TH2) system in zebrafish brain and stress activation of hypothalamic cells. *Histochem Cell Biol* 142:619–633.
- Stack A, Carrier N, Dietz D, Hollis F, Sorenson J, Kabbaj M (2010) Sex differences in social interaction in rats: role of the immediate-early gene *zif268*. *Neuropsychopharmacology* 35:570–580.
- Stednitz SJ, Washbourne P (2020) Rapid progressive social development of zebrafish. *Zebrafish* 17:11–17.
- Stednitz SJ, McDermott EM, Ncube D, Tallafuss A, Eisen JS, Washbourne P (2018) Forebrain control of behaviorally driven social orienting in zebrafish. *Curr Biol* 28:2445–2451.e3.
- Stefano L, Al Sarraj J, Rössler OG, Vinson C, Thiel G (2006) Up-regulation of tyrosine hydroxylase gene transcription by tetradecanoylphorbol

- acetate is mediated by the transcription factors Ets-like protein-1 (Elk-1) and Egr-1. *J Neurochem* 97:92–104.
- Thiel G, Schoch S, Petersohn D (1994) Regulation of synapsin I gene expression by the zinc finger transcription factor zif268/egr-1. *J Biol Chem* 269:15294–15301.
- Topilko P, Schneider-Maunoury S, Levi G, Trembleau A, Gourdji D, Driancourt MA, Rao CV, Charnay P (1998) Multiple pituitary and ovarian defects in Krox-24 (NGFI-A, Egr-1)-targeted mice. *Mol Endocrinol* 12:107–122.
- Westerfield M (2007) *The zebrafish book*, Ed 5. Eugene: Institute for Neuroscience, University of Oregon.
- Wu Z, Autry AE, Bergan JF, Watabe-Uchida M, Dulac CG (2014) Galanin neurons in the medial preoptic area govern parental behaviour. *Nature* 509:325–330.
- Yamada K, Gerber DJ, Iwayama Y, Ohnishi T, Ohba H, Toyota T, Aruga J, Minabe Y, Tonegawa S, Yoshikawa T (2007) Genetic analysis of the calcineurin pathway identifies members of the EGR gene family, specifically EGR3, as potential susceptibility candidates in schizophrenia. *Proc Natl Acad Sci USA* 104:2815–2820.
- Yamamoto K, Ruuskanen JO, Wullimann MF, Vernier P (2011) Differential expression of dopaminergic cell markers in the adult zebrafish forebrain. *J Comp Neurol* 519:576–598.
- Zhang L, Cho J, Ptak D, Leung YF (2013) The role of egr1 in early zebrafish retinogenesis. *PLoS One* 8:e56108.
- Zhang W, Tong H, Zhang Z, Shao S, Liu D, Li S, Yan Y (2018) Transcription factor EGR1 promotes differentiation of bovine skeletal muscle satellite cells by regulating MyoG gene expression. *J Cell Physiol* 233:350–362.